The ability of recycled magnetite nanoparticles to degrade carbamazepine in water through photo-Fenton oxidation at neutral pH

Anaëlle Gabet[1,2], Charlotte Guy[1], Arezou Fazli[1,3*], Hélène Métivier[2], Christine de Brauer[2], Marcello Brigante[1], Gilles Mailhot[1]

[1] Université Clermont Auvergne, CNRS, INP Clermont Auvergne, Institut de Chimie de Clermont-Ferrand, F-63000 Clermont-Ferrand, France

[2] INSA Lyon, DEEP, 34 Avenue des Arts, 69621 Villeurbanne Cedex, France

[3] Smart Materials, Istituto Italiano di Tecnologia, Via Morego 30, 16163 Genova, Italy

*Corresponding author: arezou.fazli@iit.it and arezu.fazli@yahoo.com

Abstract

Herein, the recycled magnetite obtained from industrial ferrous scrap was used as an eco-friendly, sustainable iron source in the photo-Fenton degradation of carbamazepine (CBZ), an emerging contaminant in the aqueous environment. Citrate was used as a robust chelating agent to trap and stabilize the iron required for the Fenton reaction. The results proved the formation of the Fe(III)-citrate complex, followed by the reduction of iron to Fe(II) and the formation of harmless molecules such as malonate under UV radiation. The adopted photo-Fenton process in the presence of magnetite (0.3 g L^{-1}), H_2O_2 (0.5 mM), and citrate (0.1 mM) led to about 77% degradation of CBZ. Then, degradation efficiency was improved to 99% by increasing the prior contact time between citrate and magnetite. In addition, 1 mM of citrate and 2 mM of H_2O_2 were found to be the optimal values for the degradation of CBZ under the adopted photo-Fenton process. Eventually, the experiments illustrated that the recycled magnetite could be used in the photo-Fenton process in five successive cycles without losing its efficiency.

Keywords: Carbamazepine; Photo-Fenton process; Recycled magnetite; Iron-citrate complexes, Wastewater treatment.

1. Introduction

Contaminants of emerging concern (CECs), such as drugs, pesticides, or personal care product components, are widely detected in surface waters worldwide. Wastewater treatment plant (WWTP) effluents became a significant source of CECs in the environment [1,2].

Advanced oxidation processes (AOPs) as quaternary treatments are promising for CECs removal in domestic WWTP [3]. Among them, Fenton oxidation has been studied over the past century and has demonstrated its efficacy for CECs removal in different water bodies and WWTP effluents [4]. The original Fenton process mainly consists in generating highly reactive oxygen species such as hydroxyl radicals ($^{\bullet}OH$) from H_2O_2 (HP) reactant through Fe^{2+} oxidation (Eq. (1)), followed by the Fenton-like reaction, which consists of Fe^{3+} reduction by H_2O_2 (Eq. (2)) [5].

$$Fe^{2+} + H_2O_2 \rightarrow Fe^{3+} + {}^{\bullet}OH + OH^{-} \quad (1)$$

$$Fe^{3+} + H_2O_2 \rightarrow Fe^{2+} + HO_2^{\bullet} + H^{+} \quad (2)$$

However, this degradation process faces shortcomings such as the accumulation of Fe^{+3}, which is about 6000 times less reactive than Fe^{2+} [6], and the precipitation of Fe^{3+} in the iron oxide or ferric oxyhydroxide forms above pH 3 [7]. Therefore, the process is hardly applicable to WWTPs because the effluents are generally buffered at circumneutral pH by organic matter [8]. To avoid the costs associated with the produced iron sludge and narrow pH range in homogeneous Fenton processes, the use of heterogeneous Fenton and photo-Fenton processes gained a lot of attention. In this regard, replacing soluble iron with a solid source of iron has been extensively investigated in the literature to overcome iron precipitation at neutral pH [9]. In this case, Fenton reactions can take place on the surface of the iron-containing catalysts. In addition, UV or visible light radiation could reduce ≡Fe(III) into

≡Fe(II) (Eq. (3)), enhancing the production of •OH through the Fenton reaction and, as a result, improving the oxidation procedure [10].

$$\equiv Fe(III) + H_2O \xrightarrow{h\nu} \equiv Fe(II) + {}^{\bullet}OH + H^{+} \quad (3)$$

Secondly, iron chelates were implemented as another solution to avoid iron (III) precipitation at neutral pH [11]. Citrate, ethylenediamine-N,N'-disuccinic acid (EDDS), ethylenediaminetetraacetic acid (EDTA), and nitrilotriacetic acid (NTA) have been widely reported as iron (III) chelating agents [12]. They can be used either to stabilize Fe^{+3} ions in solution or for the production of a complex of iron (≡Fe (III)) and ligand (L) on the surface of the solid iron in a heterogeneous Fenton process [13]. Moreover, because these complexes are usually highly photosensitive, they are likely to undergo reduction as defined in Eq. (4) to enhance the Fenton-like reaction.

$$[\equiv Fe\ (III)\text{-}L] \xrightarrow{h\nu} \equiv Fe\ (II) + L^{\bullet} \quad (4)$$

Magnetite (Fe_3O_4) is a mineral often found in aquifers and has both Fe^{2+} and Fe^{3+} on its reactive surface sites, favoring the occurrence of Eq. (1) and (2) [13]. The use of magnetite nanoparticles reported by Sun et al. [14] has shown encouraging results for the degradation of carbamazepine and ibuprofen at neutral pH. They demonstrated that H_2O_2 reduction into •OH mainly occurs through its adsorption on the surface of the magnetite nanoparticles. Moreover, Fe_3O_4 possesses a magnetic property that differentiates it from the recoverable catalysts used for wastewater treatment applications [15]. In our previous work, we used magnetite for hydrogen peroxide and persulfate activation to enhance sulfalene degradation at neutral pH. In the degradation process, magnetite was recovered from the reaction media and kept its activity after five cycles [15].

To improve treatment performances, Xue et al. assessed the effect of various chelating agents on the efficiency of the Fenton process implemented with magnetite and HP [16]. As

compared with magnetite alone, the oxidation rate constant of pentachlorophenol increased by 2.5 times in the presence of citrate. Citrate is a common molecule in natural water. It allows the formation of a highly biodegradable bidentate ferric complex at neutral pH which is relevant for an application in WWTP [17]. Moreover, the citrate-iron complex requires less chelating agent to be formed than complexes formed with other chelating agents [18]. However, the there is a paucity of research regarding the effect of UV irradiation on iron availability when using citrate as a chelating agent in a Fenton process with magnetite.

In the present work, for the first time, we used citrate to chelate iron from a recycled magnetite in order to develop a robust and eco-friendly photo-Fenton process. Moreover, as another novelty of this work, we investigated the fate of the complex between Fe(III) and citrate after its degradation under UV irradiation. Carbamazepine (CBZ) was chosen as a model pollutant. It is an antiepileptic drug that has raised concern during the past years because of its presence in WWTP effluents, leading to detection levels of several hundred ng L^{-1} in surface and ground waters [19,20]. The recycled magnetite was obtained from industrial ferrous scrap and was provided by a french company (Hymag'in). The influence of various contact times between magnetite and citrate for Fe(III) and citrate complex formation was evaluated. Furthermore, the efficiency of different processes such as photolysis, adsorption, photo-Fenton, and photo-Fenton-like was assessed. The optimal conditions for the photo-Fenton-like degradation process was evaluated by studying the effect of the initial pH and of the concentrations of HP, citrate, and magnetite.

2. Materials and methods

2.1. Chemicals and reagents

The recycled magnetite was obtained from Hymag'in (Saint-Martin-d'Hères, France) and the commercial one from Sigma-Aldrich. They were crushed and their structures were

analyzed by X-ray diffraction (XRD, D8 Advance, Bruker, Germany) (Fig. S1). XRD patterns confirmed the existence of magnetite particles for both commercialized and recycled samples. No specific impurity was observed in the recycled magnetite. Carbamazepine and hydrogen peroxide (H_2O_2 30% in water) were purchased from Sigma-Aldrich. Citric acid (purity > 99.5%) was provided from J.T.Baker ® brand chemistries and acetonitrile was supplied by Carlo Erba Reagents. Ultrapure water was obtained from a milli-Q system. Real wastewater was collected at the outlet of the treatment from the "3 rivières" urban WWTP, Clermont-Ferrand, France. Samples were filtered on a paper filter followed by filtration at 0.45 µm on a CHROMAFIL® Xtra RC-45/25 syringe filter from Macherey-Nagel.

2.2. Photocatalytic experiments

All the experiments were carried out in 50 mL Pyrex reactors that were placed either in the dark or in a homemade rectangular box equipped on the top with four polychromatic UVA fluorescent tubes (F15W/350BL, Sylvania Blacklight, Germany). The emission spectrum of the lamps (λ_{max} = 352 nm) was measured on top of the reactors with an optical fiber and a charge-coupled device spectrophotometer (Ocean Optics USD 2000 + UV-vis), calibrated using a DH-2000-CAL Deuterium Tungsten Halogen reference lamp (Fig. S2).

CBZ stock solution (100 µM) was prepared in ultrapure water and stored in the dark at 4°C. Predetermined amounts of magnetite and citric acid were added to 50 mL of ultrapure water and stirred at 1500 rpm for various durations in the dark before the addition of HP and carbamazepine (5 µM) at time 0. After adding CBZ and HP, the solutions were set into the UVA reactor and the photodegradation processes were launched. 900 µL were withdrawn and filtered at fixed times from the reactor and mixed with 100 µL of methanol to inhibit any further degradation reaction.

Carbamazepine concentrations were followed using a Waters Acquity Ultra-High-Performance Liquid Chromatography (UPLC) system equipped with a BEH C18 column (100 × 2.1 mm, 1.7 µm), coupled to a diode array detector (200-400 nm) and a fluorescence detector (λ_{ex} = 280 nm, λ_{em} = 305 nm). The initial CBZ concentration of 5 µM does not require pre-concentration before UPLC analysis, avoiding a source of error. An isocratic method was used over 3 minutes. The elution flow rate was 0.6 mL min^{-1} and eluent was a mixture of milli-Q water (70%) and acetonitrile (30%). The injection volume was 10 µL and the column temperature was fixed at 40°C.

The following first-order equation fitted the concentration of CBZ during the radiation:

$$C_t/C_0 = \exp\ (-k't)$$

Where C_0 and C_t are respectively the initial concentration of CBZ and the concentration at time t, while k' is the pseudo-first-order rate constant. Error bars representing ± one standard deviation were calculated as the mean of two measurements.

2.3. Determination of HP and Iron (II) concentrations

UV-visible spectra were measured and recorded with a Cary 300 scan UV-visible spectrophotometer. HP concentration was followed using p-hydroxyphenyl acetic acid (HPAA, purity > 98%) and horseradish peroxidase (POD), according to a spectrofluorimetric quantification method [21] with a Varian Cary Eclipse fluorescence spectrophotometer. The excitation wavelength was set at 320 nm. The measured formation of the HPAA dimer was correlated with the HP concentration using standard solutions.

Iron (II) was quantified with ferrozine (3-(2-pyridyl)-5,6-bis(4-phenyl sulfonic acid)-1,2,4-triazine), a colorimetric complexant. The molar absorption coefficient of the colored ferrozine-iron (II) complex at 562 nm ($\varepsilon_{562\ nm}$ = 27 900 M^{-1} cm^{-1}) was used to calculate dissolved iron concentration in solution.

2.4. Laser flash photolysis

Time-resolved spectroscopy was used to determine the second-order rate constant between the hydroxyl radical and CBZ. The experiment was carried out with the fourth harmonic (λ_{exc} = 266 nm) of a quanta ray GCR 130-01 Nd:YAG laser system instrument and an energy of 45 mJ/pulse. The experimental setup has been described before [22].

2.5. IC-MS analysis

Ionic species were identified and quantified using a Thermo Fisher Scientific with Dionex ICS 6000 ionic chromatography and a simple quadrupole ISQ-EC mass detector with electrospray ionization (ESI). The column used was an Ion Pac AS11-HC 4 µm with a size of 2 × 250 mm and the precolumn was an AG11-HC 4 µm (2 × 50 mm). The eluent was a gradient of KOH from 1 to 60 mM during 30 min at a flow rate of 0.36 mL min^{-1}.

3. Results and discussion

3.1. Ferric-citrate complex

3.1.1. Formation and photoreactivity of the ferric-citrate complex

According to the literature, one of the main challenges regarding the photo-Fenton process is its implementation at circumneutral pH for pollutant degradation. Fig. 1 (a) shows the absorption spectra of Fe(III) and of the Fe(III)-citrate complex in the wavelength range of 200 to 500 nm. According to the presented results, the Fe(III)-citrate complex formation allowed to extend the light absorbance in the visible range compared to the sole Fe(III). Therefore, the formation and stability of the ferric-citrate complex (near circumneutral pH) are of great importance. The production of the ferric-citrate complex as a function of time at pH 7 was evaluated and results were reported in Fig. 1 (b). The formation of the complex at pH 7 was

confirmed and its concentration was seen to increase with the contact time between magnetite and citrate.

Clarizia et al. [12] also demonstrated that the generated ferric-citrate complex enhanced the UV–vis light absorbance during the homogenous photo-Fenton process, resulting in improved photochemical reductions. Therefore, before studying the performance of the photo-Fenton process in the presence of the recycled magnetite and citrate as a ligand, some control experiments were carried out to understand the behavior of the ferric-citrate complex under UVA radiation (Fig. 1(c)). The results showed that the ferric-citrate complex was decomposed under the radiation. According to the literature review, the photoreactivity of ferric-carboxylate complexes depends on the nature of the ligand. Citrate is a di-carboxylate ligand that can coordinate iron centers, increasing the ligand-to-metal charge transfer (LMCT) absorption band [23,24]. This band, in the excited state, leads to a photoredox process where the ligand is oxidized while the metal is reduced (Eq. 4) [25]. Therefore, the photolysis of the ferric-citrate complex, with the assistance of the LMCT process, leads to the production of Fe (II) and ligand radicals. Then, the subsequent Fenton reactions with the added HP and the photo-generated Fe (II) allows for the generation of hydroxyl radicals ($^{\bullet}OH$) [26]. Moreover, in the presence of O_2, the oxidized citrate ligand radical leads to the production of the superoxide radical anion ($O_2^{\bullet-}$) that is in acid-base equilibrium with $HO_2^{\bullet}$ [26].

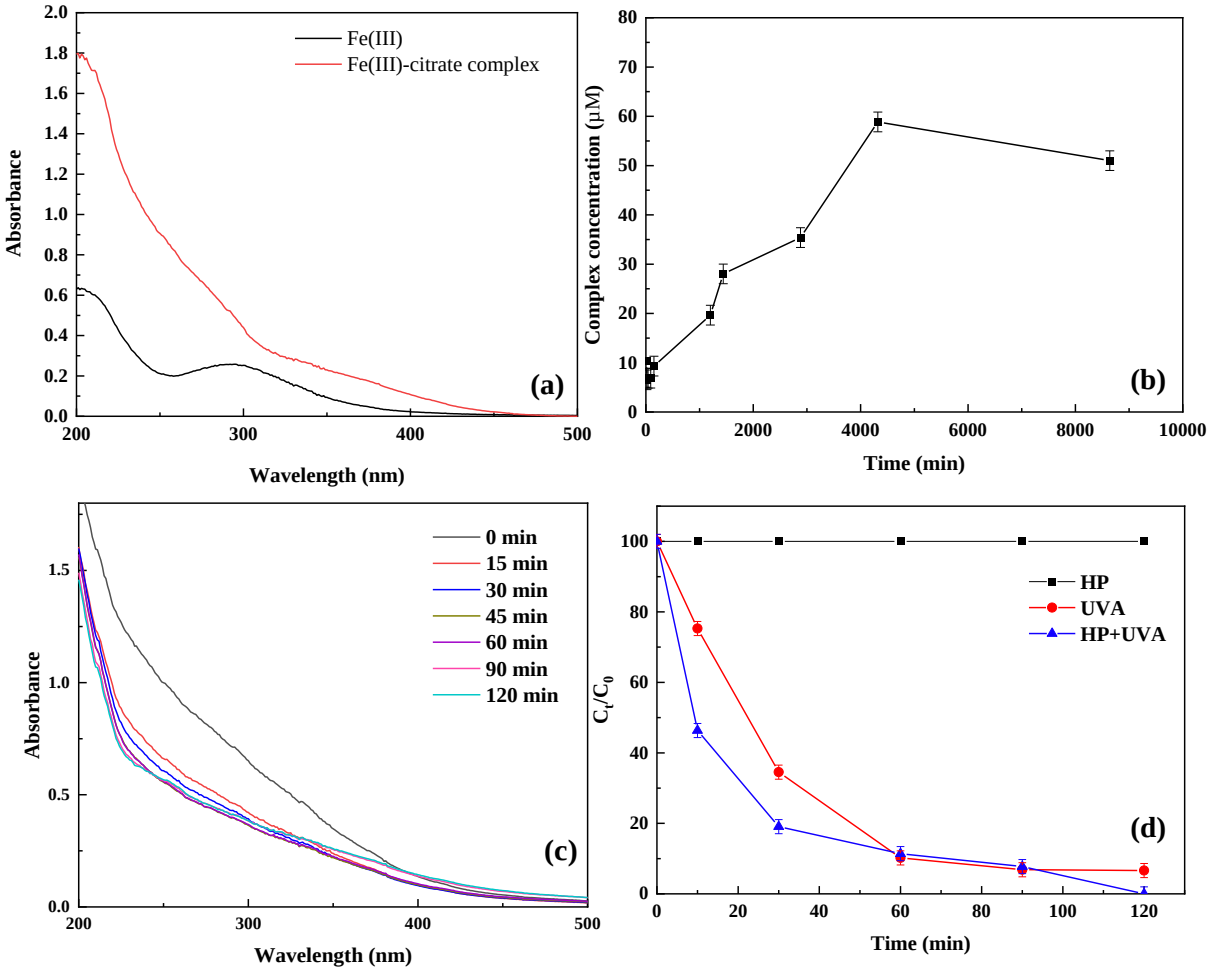

Fig. 1. (a) UV-visible spectra of Fe (III) and of the Fe (III)-citrate complex at natural pH (≈ 3), (b) formation of the Fe (III)-citrate complex in the presence of magnetite (pH = 7.0), (c) UV-visible spectra of the Fe (III)-citrate complex during UVA radiation between 0 and 120 minutes, pH = 7.0, and (d) the degradation of citrate in different systems: sole UVA, sole HP, and HP/UVA (pH = 7.0). Fe(III) = 0.2 mM, [Fe(III)-citrate] = 0.2 mM and [HP] = 0.2 mM.

3.1.2. Fate of the ferric-citrate complex during photodegradation

One of the topics which have not yet been well addressed in AOPs involving organic iron complexes is the fate of the organic complex during the photochemical process. For this purpose, the photodegradation of citrate as Fe (III) chelating agent was followed. Fig. 1 (d)

shows the degradation of citrate with and without UVA irradiation. The results showed complete degradation of citrate after 2 hours under UVA radiation. Furthermore, this degradation was accelerated in the presence of HP (0.2 mM). Nonetheless, no degradation was observed in the presence of HP without UVA radiation after two hours. With a view to applying this process in a WWTP, it is important to know the fate of the complexing agent (citric acid) during the photochemical reaction. Therefore, a study on the photodegradation products, in the presence or absence of HP, was conducted by ion chromatography coupled to mass spectrometry (IC-MS).

Several peaks have been identified on the IC-MS chromatograms (Fig. S3), revealing the formation of various organic compounds such as acetate, formate or malonate, among which malonate was observed to be the main by-product. Its generation was evaluated in the presence and absence of HP under UVA radiation (Fig. S4). Accordingly, its concentration was lower in the presence of HP. By considering these results and those found in the literature presenting mechanisms for the degradation of Fe(III) organic complexes, a mechanism was proposed for the degradation of the Fe(III)-citrate complex during the photo oxidation-reduction process (Fig. 2) [27].

The complex undergoes degradation via two reaction pathways ((1) and (2)) following its UVA absorption and the LMCT phenomenon. The dissociation of the complex from the carboxyl group results in the formation of carboxyl radicals. This can be followed by the decarboxylation of the previously formed carboxyl radicals, leading to the generation of carbon-centered radicals ((3) and (4)). These are unstable and react with the available molecular oxygen giving rise to the formation of peroxide radicals ((5) and (6)). Then, the produced intermediates degrade to form alkoxy radicals and oxygen ((7) and (8)). On the one hand, the β-scission of the C–H bond occurs to generate aldehyde ((9)). On the other hand, the scission of the C-C bond produces a new carbon-centered radical ((10)), which in turn reacts

with an oxygen molecule to form either the malonic acid ((11)) or acetone dicarboxylic acid ((12)). Furthermore, the produced alkoxy radicals can directly lead to the formation of the same by-products ((13) and (14)).

Considering the proposed mechanism, carboxylic acids like succinic acid were degraded by a similar mechanism, leading mainly to the formation of other carboxylic acids of a shorter carbon chain length [28]. Therefore, citric acid decomposes into less harmful molecules, validating its use as a chelating agent of Fe (III) towards a large-scale implementation of photo-Fenton processes with the aim of sustainable development.

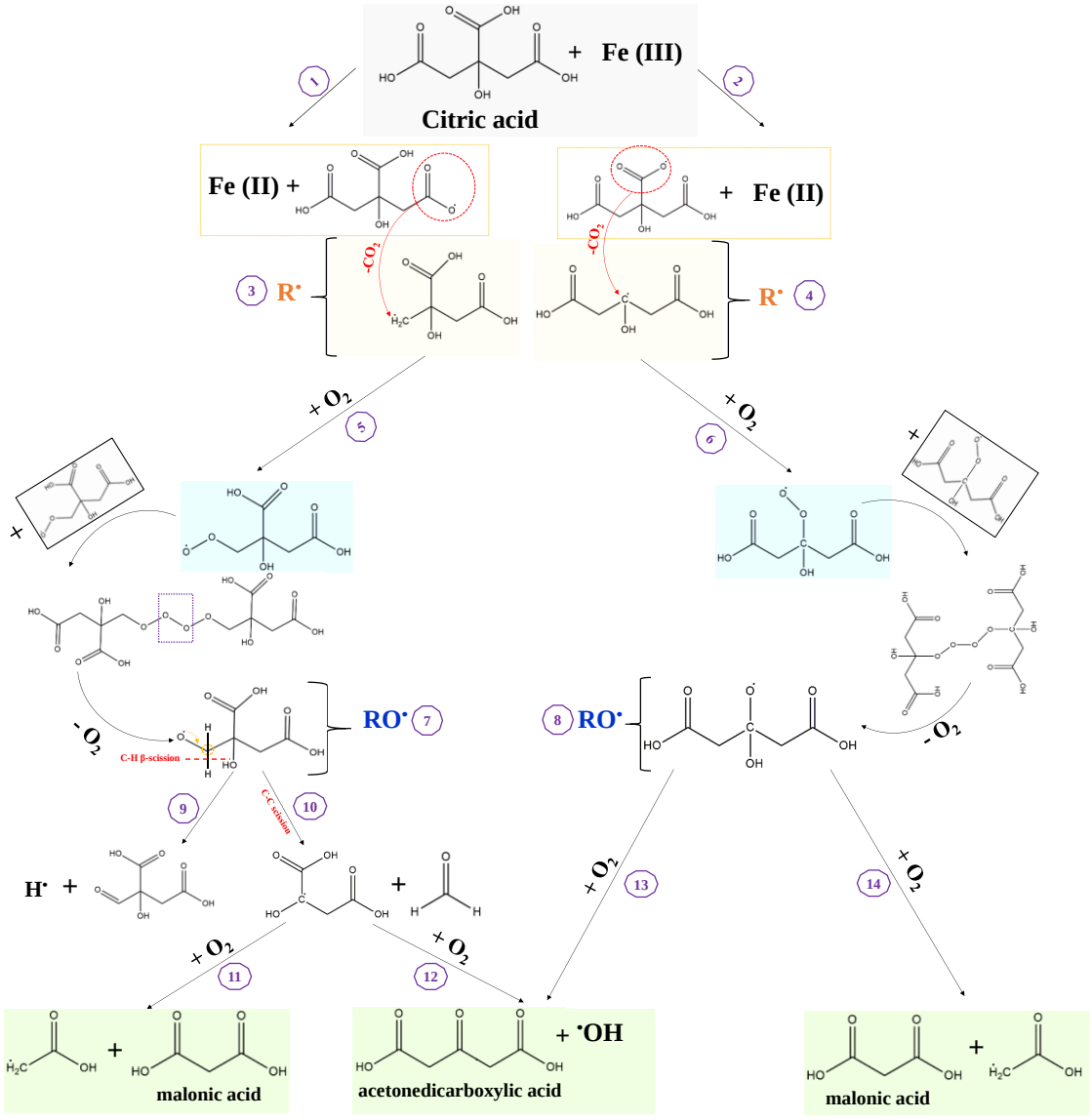

Fig. 2. Degradation mechanism of the Fe(III)-citrate complex.

3.2. CBZ degradation by photo-Fenton process

After characterizing the generated Fe(III)-citrate complex in the presence of the recycled magnetite, the photocatalytic activity of the generated complex was studied. In Fig. 3, CBZ degradation is followed under various conditions.

Under UVA radiation, no photolysis was observed. Furthermore, in the presence of magnetite (0.3 g L^{-1}) and H_2O_2 (0.5 mM), the oxidation of CBZ was very low, and only 10% of CBZ degraded after 4 hours. Nevertheless, under identical reaction conditions, the efficiency of CBZ degradation increased by 26% after 4 hours of exposure to UVA irradiation. The production of hydroxyl radicals (•OH) through H_2O_2 photolysis could be the primary reason for the increased degradation efficiency observed during exposure to UVA irradiation. This finding was validated through additional supplementary experiments. Fig. 3 illustrates that in the absence of magnetite under the same reaction conditions, CBZ degradation was discovered to be more efficient, resulting in a degradation rate of 40% after 4 hours. This is due to the photolysis of H_2O_2 by UVA radiation, which produces highly reactive hydroxyl radicals (•OH). H_2O_2 photolysis constant ($k'_{H_2O_2}$) was determined to be $1.48 \pm 0.07 \times 10^{-6}$ s^{-1}, and the second-order rate constant between CBZ and •OH ($k''_{CBZ,OH}$) was found to be 1.99×10^{10} M^{-1} s^{-1}. However, upon comparing the degradation results of CBZ for UVA/magnetite/HP and UVA/HP, it can be observed that the presence of magnetite did not lead to an improvement in degradation efficiency. This finding suggests that the use of recycled magnetite at neutral pH in combination with H_2O_2 does not appear to induce the Fenton reaction. Based on the results presented in Fig. S5, it is noticeable that negligible amounts of dissolved iron were measured, indicating the low contribution of both homogeneous and heterogeneous photo-Fenton reactions in the CBZ degradation process.

On the contrary, in the presence of citrate (0.1 mM), magnetite (0.3 g L^{-1}), H_2O_2 (0.5 mM), and UVA irradiation the CBZ degradation efficiency was elevated to 77%. An increase in degradation efficiency is attributed to the formation of Fe(III)-citrate complex on the magnetite surface. Within the 7-7.5 pH range, more than 95% citrate is under the Cit^{3-} form [29]. According to Hamm et al. [30], citrate-iron chelates are formed at neutral pH. This photosensitive complex can be degraded under UVA radiation, improving the Fenton-like reactions. It is worth noting that the magnetite/citrate/HP and magnetite/citrate/UVA processes did not show a significant effect on the degradation of CBZ (the results were not presented in Fig. 3). Thus, the photolysis of the Fe(III)-citrate plays a significant role in the degradation of CBZ.

In addition, it is worth noting that iron can also be released into water from the generated Fe-L complexes, which can lead to the homogeneous Fenton-like oxidation of contaminants [31]. Therefore, further experiments were conducted to assess the contribution of both homogeneous and heterogeneous photo-Fenton-like processes to the degradation of CBZ. Fig. S5 shows the concentration of the leached iron from the surface complex that was generated. Thus, it can be inferred that the degradation of CBZ is associated with a combination of both heterogeneous and homogeneous Fenton-like reactions. However, it should be noted that the total concentration of iron in magnetite (0.3 g L^{-1}) was about 400 µM, while the dissolved concentration of Fe (II) and Fe (III) was found to be no more than 5 µM. This result suggests the low contribution of homogeneous photo-Fenton reactions to the degradation process.

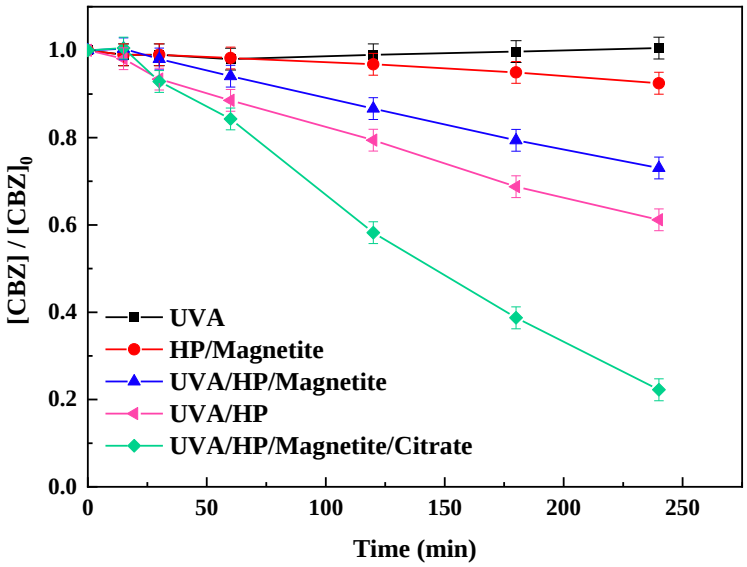

Fig. 3. Degradation of carbamazepine under various processes. Experimental conditions: [magnetite] = 0.3 g L^{-1}, [CBZ] = 5 µM, [HP] = 0.5 mM, [citrate] = 0.1 mM, and pH = 7.5 ± 0.2.

3.3. Influence of the contact time between citric acid and magnetite

The contact time between magnetite and citric acid in an aqueous solution prior to the photochemical reaction plays a key role in the iron-citrate complex formation, which is favorable for the degradation of CBZ. Fig. 4 compares the degradation of CBZ under the magnetite/citrate/HP process when the contact time between magnetite and citric acid varies from 1 hour to 4 and 24 hours. These results clearly show that in the range from 0 to 24 hours, the higher the contact time, the faster the degradation of CBZ. It is therefore necessary to allow enough time for citric acid and iron from magnetite to form complexes [18] and further experiments were carried out with a contact time of 24 hours between magnetite and citric acid prior to the photochemical reaction.

Nonetheless, further experiments allowed to observe that the process efficiency significantly decreased with a longer contact time of 48 hours. Because they were carried out in different conditions, it should be noted that the corresponding results are not included in

Fig. 4. However, they are valuable for understanding the relationship between contact time and CBZ degradation rate. According to a literature review [32], the Fe-L complex could inhibit the decomposition of H_2O_2 by competing for the available active sites on the surface of magnetite. Hence, the slower decomposition of H_2O_2 results in reduced production of hydroxyl radicals, which can limit the effectiveness of pollutant degradation. Thus, in our case, the reduced degradation efficiency observed with a longer contact time could be attributed to the increased production of surface complexes, which could impede the adsorption of H_2O_2 and thereby decrease the production of active radicals required for the degradation of CBZ.

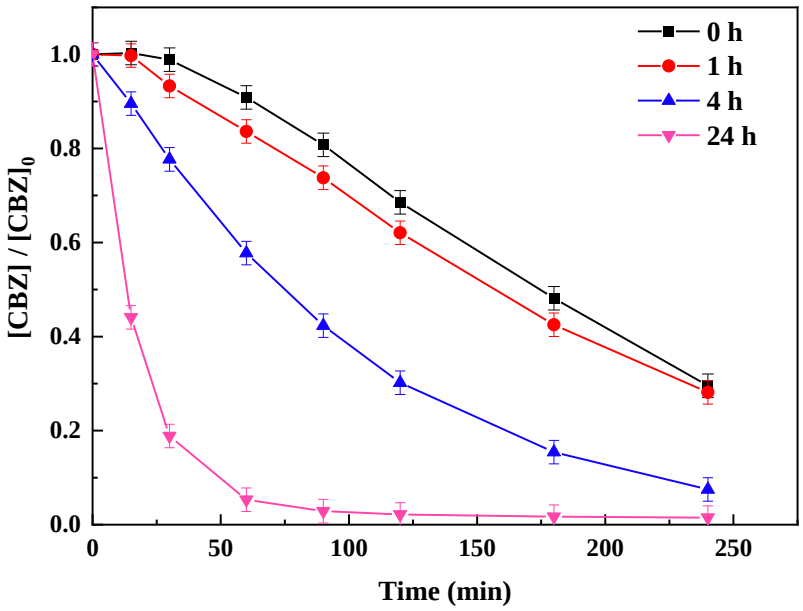

Fig. 4. Degradation of carbamazepine using various citrate-magnetite contact time. Experimental conditions: [magnetite] = 0.3 g L^{-1}, [CBZ] = 5 µM, [HP] = 0.5 mM, [citrate] = 0.1 mM and pH = 7.5 ± 0.2.

3.4. Influence of different parameters on the degradation of CBZ

It was previously seen that the initial citric acid concentration played an essential role in the formation of the iron-citrate complex [33]. On the other hand, it should be verified

whether the initial citric acid concentration also has an impact on the degradation of CBZ. Fig. 5 (a) depicts the variation of CBZ concentration in the presence of various citric acid concentrations (0.1, 0.5, 1, 1.5, and 2 mM). The results highlight the existence of a maximum citric acid concentration (1 mM) for complex formation optimisation towards faster degradation of carbamazepine. An excessive amount of citric acid (> 1 mM) showed the opposite effect on the degradation of CBZ. The reduced degradation efficiency can be attributed to the competition between citric acid and CBZ to react with the generated hydroxyl radicals.

According to the literature review [34], the Fenton reaction requires the addition of hydrogen peroxide. Therefore, the concentration of HP is one of the other main parameters to be considered. Fig. 5 (b) represents the influence of various HP concentrations on the degradation of CBZ under the photo-Fenton process. It can be seen that in the presence of magnetite and citrate only, carbamazepine is degraded by approximately 20%, whereas the addition of HP significantly increases process efficiency. Thus, the addition of 1 mM of hydrogen peroxide degrades CBZ by more than 50% after 2 hours of irradiation. However, it is evident that there is a limit HP concentration in the studied conditions, beyond which the reaction between hydrogen peroxide and $^{\bullet}OH$ will be too important and lead to slower degradation of CBZ [35]. We observed that increasing the concentration of HP from 2 mM to 3 mM resulted in only a 19% difference in degradation efficiency, however, 2 mM was chosen as the optimal concentration to avoid the need for additional chemicals in the process.

Previous research has shown that the Fenton reaction is optimal at pH 3 [36], whereas domestic WWTP effluents are usually at circumneutral pH. Fig. 5 (c) shows the degradation of CBZ at pH 3.5 and 7.5 in the dark and under UVA radiation. In the absence of light, almost no degradation of CBZ was observed at both pH values. In the presence of light, the degradation of CBZ is very similar between both pH values during the first hour of

irradiation. After that, the degradation of CBZ slows down at pH 7.5 whereas it continues at acidic pH (3.5). This can be due to the precipitation of iron at pH 7.5 after the photoredox process observed with the Fe(III)-citrate complex. At pH 3.5 on the other hand, Fe(II) generated from the photoredox process can be oxidized into Fe(III) and a new photoredox process can be obtained from Fe(III)-aqua complexes. However, it can be deduced that pH variation does not affect the initial degradation rate of CBZ.

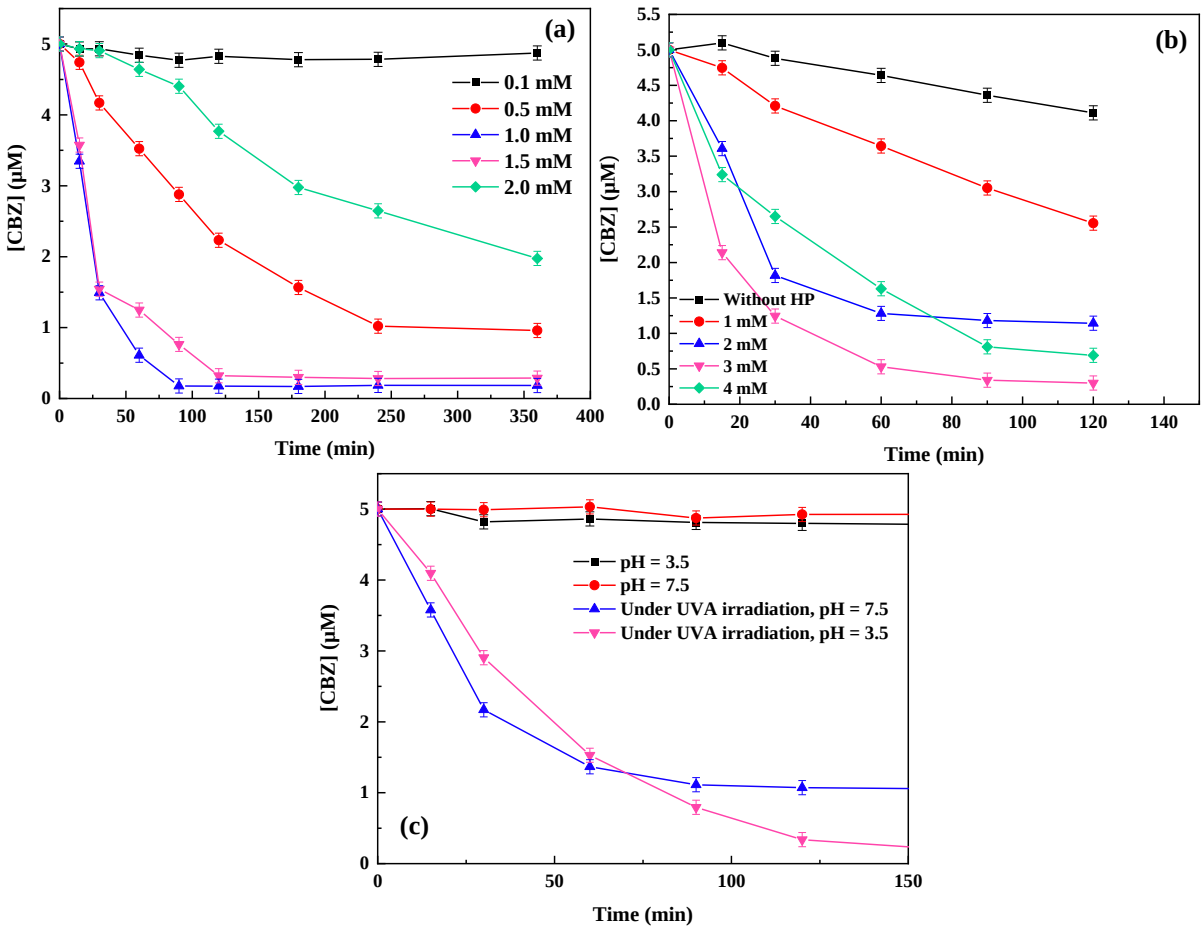

Fig. 5. Effect of (a) citrate concentration, (b) HP concentration, and (c) the solution pH on the degradation of CBZ under the photo-Fenton degradation process. The contact time between magnetite and citric acid is equal to 24h. Experimental conditions: [magnetite] = 0.1 g L^{-1}, [CBZ] = 5 µM, [HP] = 1 mM, and pH = 7.5 ± 0.2.

3.5. Efficiency and reusability of the recycled magnetite

One of the main scopes of this research study was to prove that the recycled magnetite from iron scrap could be revalorized in a wastewater treatment process. Recycled and commercial magnetite samples were purchased from Hymag'in and Sigma-Aldrich. Their characterization is presented in Table. 1.

Table. 1. Characterization of the provided magnetite.

	Recycled magnetite	**Commercial magnetite**
Particle size (nm)	~ 320	50-100
Fe^{II}/Fe^{III}	0.26 (surface)	Unknown
Specific surface area ($m^2 g^{-1}$)	4.3	20-50
Iron content	96.3%	> 97%

As seen in Fig. 6 (a), the recycled magnetite allowed for a degradation of CBZ around five times higher in our experimental conditions than the commercial magnetite supplied by Sigma-Aldrich, although the latter has a smaller particle size and from 5 to 12 times higher specific surface area. Therefore, a large specific surface area does not seem to play a major role in the degradation rate of CBZ. The Fe^{II}/Fe^{III} ratio on the surface of magnetite is usually close to 0.5. However, that of the recycled magnetite, which has undergone surface oxidation, is 0.26 (Table 1). Thus, its higher efficiency is attributed to a larger Fe^{III} fraction at its surface, available for citrate complexation.

Then, the performance of the recycled magnetite was monitored in five successive photo-Fenton cycles. Fig. 6 (b) displays CBZ degradation rates in the presence of the recycled magnetite during the first cycle and after five degradation cycles. It is seen that the degradation of CBZ followed similar trends in both conditions and it was even faster during the fifth degradation cycle. After 2 hours of irradiation, CBZ was degraded by more than

30% in the first cycle whereas it was degraded by more than 50% after five degradation cycles. This shows that the recycled magnetite is able to provide similar or higher efficiency for a certain period.

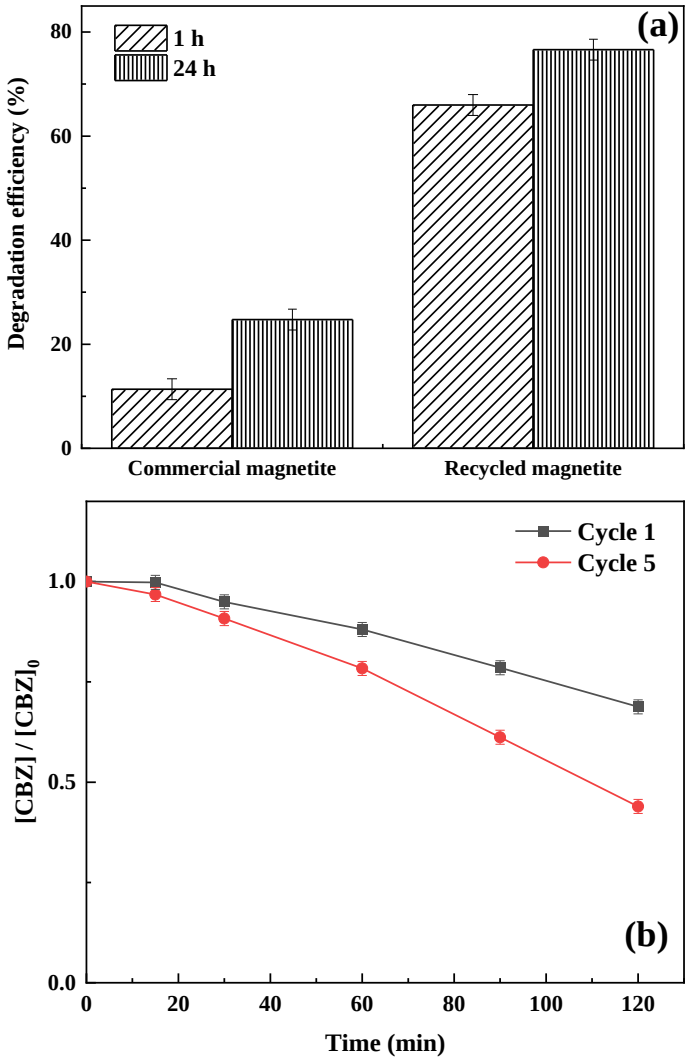

Fig. 6. (a) Photo-Fenton degradation of CBZ in the presence of a recycled magnetite from iron scrap or of a commercial magnetite (Sigma-Aldrich) after 24h contact time between citrate and magnetite prior to the reaction. (b) Performance of the recycled magnetite after five cycles of photo-Fenton process. Experimental conditions: [magnetite] = 0.3 g L^{-1}, [CBZ] = 5 µM, [HP] = 0.5 mM, and pH = 7.5 ± 0.2.

The proposed technology has several practical implications. First, using recycled magnetite instead of new magnetite can significantly reduce the cost of the treatment process by minimizing the need for new raw materials and reducing waste generation. Furthermore, recycled magnetite has shown higher efficiency and consistent performance over several cycles compared to commercial magnetite, making it a suitable alternative for the treatment of recalcitrant contaminants. Additionally, citrate, a biodegradable and inexpensive chelating agent, can form stable complexes with iron, which can prevent the formation of unwanted iron precipitates that can interfere with the photo-Fenton process. This, in turn, can improve the efficiency and effectiveness of the process. Consequently, by coupling recycled magnetite with citrate, the technology becomes a cost-effective and sustainable choice for large-scale photo-Fenton processes, capable of effectively removing organic contaminants from wastewater while minimizing environmental impact.

4. Conclusion

In this work, the photo-Fenton process was implemented using recycled magnetite as a solid source of iron in order to add new merit to industrial ferrous scrap. Additionally, citric acid was presented as an environmentally friendly Fe (III) chelating agent for the formation of a photo-labile Fe (III)-citrate complex, which allowed for the photo-Fenton process to be carried out at a neutral pH. Carbamazepine was used as a model pollutant to assess the process efficiency. First, the photo-degradation of the Fe (III)-citrate complex under UVA radiation was observed to generate Fe(II) to feed the Fenton reaction and produce hydroxyl radicals for CBZ degradation. Moreover, the degradation of the ligand under radiation did not result in toxic compounds, demonstrating the environmental compatibility of the process. In this regard, a degradation mechanism of the citrate ligand to malonic and acetonedicarboxylic acids was proposed.

It is worth noting that, after four hours of UVA exposure, the concentration of CBZ decreased by 77% in the photo-Fenton process implemented with citrate (0.1 mM), hydrogen peroxide (0.5 mM), and magnetite (0.3 g L^{-1}). This efficienct performance was ascribed to the reaction between Fe (II), generated by the photolysis of the Fe(III)-citrate complex, and the added H_2O_2, which produces the highly oxidative hydroxyl radicals throughout the Fenton reaction. Then, process efficiency was optimized by increasing the concentration of citrate to 1 mM and hydrogen peroxide to 3 mM. For both reactants, maximum concentrations were determined. Excessive hydroxyl radical production, which could react with hydrogen peroxide and adversely affect the efficiency of the process, was likely at higher concentrations. Moreover, increasing the prior contact time between magnetite and citrate up to 24 hours accelerated the degradation rate of CBZ. Finally, relatively constant efficiency of the recycled magnetite was observed over five photo-Fenton cycles, showing great Fe (III) availability for complexation and encouraging results towards an application in WWTPs. Due to the ability of this recycled magnetite, coupled with citric acid, to implement the photo-Fenton process under mild conditions, this work may provide insight into building sustainable and large-scale processes for the removal of organic micropollutants in secondary domestic effluents or industrial effluents.

Acknowledgments

We acknowledge the French Embassy in Iran, the project I-Site CAP 20-25, the program PAUSE of collège de France, and PAI (Pack Ambition Recherche) SOLDE from the Region Auvergne Rhône Alpes for the financial support of Arezou Fazli in this project. The authors wish to acknowledge also the financial support of the “Région Auvergne-Rhône-Alpes” for their financial support through the “Pack Ambition Recherche”. The authors also thank Hymag’in for providing the recycled magnetite.

References

[1] A. Fazli, M. Brigante, A. Khataee, G. Mailhot, $Fe_{2.5}Co_{0.3}Zn_{0.2}O_4$/CuCr-LDH as a visible-light-responsive photocatalyst for the degradation of caffeine, bisphenol A, and simazine in pure water and real wastewater under photo-Fenton-like degradation process, Chemosphere. (2021) 132920. https://doi.org/10.1016/j.chemosphere.2021.132920.

[2] T.K. Kasonga, M.A.A. Coetzee, I. Kamika, V.M. Ngole-Jeme, M.N. Benteke Momba, Endocrine-disruptive chemicals as contaminants of emerging concern in wastewater and surface water: A review, Journal of Environmental Management. 277 (2021) 111485. https://doi.org/10.1016/j.jenvman.2020.111485.

[3] D.B. Miklos, C. Remy, M. Jekel, K.G. Linden, J.E. Drewes, U. Hübner, Evaluation of advanced oxidation processes for water and wastewater treatment – A critical review, Water Research. 139 (2018) 118–131. https://doi.org/10.1016/j.watres.2018.03.042.

[4] E. Brillas, Fenton, photo-Fenton, electro-Fenton, and their combined treatments for the removal of insecticides from waters and soils. A review, Separation and Purification Technology. 284 (2022) 120290. https://doi.org/10.1016/j.seppur.2021.120290.

[5] N. Thomas, D.D. Dionysiou, S.C. Pillai, Heterogeneous Fenton catalysts: A review of recent advances, Journal of Hazardous Materials. 404 (2021) 124082. https://doi.org/10.1016/j.jhazmat.2020.124082.

[6] L. Wu, W. Wang, S. Zhang, D. Mo, X. Li, Fabrication and Characterization of Co-Doped Fe_2O_3 Spindles for the Enhanced Photo-Fenton Catalytic Degradation of Tetracycline, ACS Omega. 6 (2021) 33717–33727. https://doi.org/10.1021/acsomega.1c04950.

[7] M.M. Bello, A.A. Abdul Raman, A. Asghar, A review on approaches for addressing the limitations of Fenton oxidation for recalcitrant wastewater treatment, Process Safety and

Environmental Protection. 126 (2019) 119–140. https://doi.org/10.1016/j.psep.2019.03.028.

[8] P. Soriano-Molina, P. Plaza-Bolaños, A. Lorenzo, A. Agüera, J.L. García Sánchez, S. Malato, J.A. Sánchez Pérez, Assessment of solar raceway pond reactors for removal of contaminants of emerging concern by photo-Fenton at circumneutral pH from very different municipal wastewater effluents, Chemical Engineering Journal. 366 (2019) 141–149. https://doi.org/10.1016/j.cej.2019.02.074.

[9] H. Guo, Z. Li, Y. Zhang, N. Jiang, H. Wang, J. Li, Degradation of chloramphenicol by pulsed discharge plasma with heterogeneous Fenton process using Fe_3O_4 nanocomposites, Separation and Purification Technology. 253 (2020) 117540. https://doi.org/10.1016/j.seppur.2020.117540.

[10] Y. Wu, X. Li, H. Zhao, F. Yao, J. Cao, Z. Chen, F. Ma, D. Wang, Q. Yang, 2D/2D FeNi-layered double hydroxide/bimetal-MOFs nanosheets for enhanced photo-Fenton degradation of antibiotics: Performance and synergetic degradation mechanism, Chemosphere. 287 (2022) 132061. https://doi.org/10.1016/j.chemosphere.2021.132061.

[11] W. Huang, M. Brigante, F. Wu, K. Hanna, G. Mailhot, Effect of ethylenediamine-N,N′-disuccinic acid on Fenton and photo-Fenton processes using goethite as an iron source: optimization of parameters for bisphenol A degradation, Environ Sci Pollut Res. 20 (2013) 39–50. https://doi.org/10.1007/s11356-012-1042-6.

[12] L. Clarizia, D. Russo, I. Di Somma, R. Marotta, R. Andreozzi, Homogeneous photo-Fenton processes at near neutral pH: A review, Applied Catalysis B: Environmental. 209 (2017) 358–371. https://doi.org/10.1016/j.apcatb.2017.03.011.

[13] D. Jia, S.-P. Sun, Z. Wu, N. Wang, Y. Jin, W. Dong, X.D. Chen, Q. Ke, TCE degradation in groundwater by chelators-assisted Fenton-like reaction of magnetite: Sand

columns demonstration, Journal of Hazardous Materials. 346 (2018) 124–132. https://doi.org/10.1016/j.jhazmat.2017.12.031.

[14] S.-P. Sun, X. Zeng, C. Li, A.T. Lemley, Enhanced heterogeneous and homogeneous Fenton-like degradation of carbamazepine by nano-Fe_3O_4/H_2O_2 with nitrilotriacetic acid, Chemical Engineering Journal. 244 (2014) 44–49. https://doi.org/10.1016/j.cej.2014.01.039.

[15] A. Fazli, A. Khataee, M. Brigante, G. Mailhot, Cubic cobalt and zinc co-doped magnetite nanoparticles for persulfate and hydrogen peroxide activation towards the effective photodegradation of Sulfalene, Chemical Engineering Journal. 404 (2021) 126391. https://doi.org/10.1016/j.cej.2020.126391.

[16] X. Xue, K. Hanna, C. Despas, F. Wu, N. Deng, Effect of chelating agent on the oxidation rate of PCP in the magnetite/H_2O_2 system at neutral pH, Journal of Molecular Catalysis A: Chemical. 311 (2009) 29–35. https://doi.org/10.1016/j.molcata.2009.06.016.

[17] Y. Zhang, M. Zhou, A critical review of the application of chelating agents to enable Fenton and Fenton-like reactions at high pH values, Journal of Hazardous Materials. 362 (2019) 436–450. https://doi.org/10.1016/j.jhazmat.2018.09.035.

[18] U.J. Ahile, R.A. Wuana, A.U. Itodo, R. Sha'Ato, R.F. Dantas, A review on the use of chelating agents as an alternative to promote photo-Fenton at neutral pH: Current trends, knowledge gap and future studies, Science of The Total Environment. 710 (2020) 134872. https://doi.org/10.1016/j.scitotenv.2019.134872.

[19] J.M. Galindo-Miranda, C. Guízar-González, E.J. Becerril-Bravo, G. Moeller-Chávez, E. León-Becerril, R. Vallejo-Rodríguez, Occurrence of emerging contaminants in environmental surface waters and their analytical methodology – a review, Water Supply. 19 (2019) 1871–1884. https://doi.org/10.2166/ws.2019.087.

[20] Q. Sui, X. Cao, S. Lu, W. Zhao, Z. Qiu, G. Yu, Occurrence, sources and fate of pharmaceuticals and personal care products in the groundwater: A review, Emerging Contaminants. 1 (2015) 14–24. https://doi.org/10.1016/j.emcon.2015.07.001.

[21] W.L. Miller, D.R. Kester, Hydrogen peroxide measurement in seawater by (p-hydroxyphenyl)acetic acid dimerization, Anal. Chem. 60 (1988) 2711–2715. https://doi.org/10.1021/ac00175a014.

[22] A. Gabet, H. Métivier, C. de Brauer, G. Mailhot, M. Brigante, Hydrogen peroxide and persulfate activation using UVA-UVB radiation: Degradation of estrogenic compounds and application in sewage treatment plant waters, Journal of Hazardous Materials. 405 (2021) 124693. https://doi.org/10.1016/j.jhazmat.2020.124693.

[23] T.-W. Chang, H. Ko, W.-S. Huang, Y.-C. Chiu, L.-X. Yang, Z.-C. Chia, Y.-C. Chin, Y.-J. Chen, Y.-T. Tsai, C.-W. Hsu, C.-C. Chang, P.-J. Tsai, C.-C. Huang, Tannic acid-induced interfacial ligand-to-metal charge transfer and the phase transformation of Fe_3O_4 nanoparticles for the photothermal bacteria destruction, Chemical Engineering Journal. 428 (2022) 131237. https://doi.org/10.1016/j.cej.2021.131237.

[24] J. Chen, W.R. Browne, Photochemistry of iron complexes, Coordination Chemistry Reviews. 374 (2018) 15–35. https://doi.org/10.1016/j.ccr.2018.06.008.

[25] M. Passananti, V. Vinatier, A.-M. Delort, G. Mailhot, M. Brigante, Siderophores in Cloud Waters and Potential Impact on Atmospheric Chemistry: Photoreactivity of Iron Complexes under Sun-Simulated Conditions, Environ. Sci. Technol. 50 (2016) 9324–9332. https://doi.org/10.1021/acs.est.6b02338.

[26] C. Ruales-Lonfat, J.F. Barona, A. Sienkiewicz, J. Vélez, L.N. Benítez, C. Pulgarín, Bacterial inactivation with iron citrate complex: A new source of dissolved iron in solar photo-Fenton process at near-neutral and alkaline pH, Applied Catalysis B: Environmental. 180 (2016) 379–390. https://doi.org/10.1016/j.apcatb.2015.06.030.

[27] S. Jaber, M. Leremboure, V. Thery, A.-M. Delort, G. Mailhot, Mechanism of photochemical degradation of Fe(III)-EDDS complex, Journal of Photochemistry and Photobiology A: Chemistry. 399 (2020) 112646. https://doi.org/10.1016/j.jphotochem.2020.112646.

[28] T. Charbouillot, S. Gorini, G. Voyard, M. Parazols, M. Brigante, L. Deguillaume, A.-M. Delort, G. Mailhot, Mechanism of carboxylic acid photooxidation in atmospheric aqueous phase: Formation, fate and reactivity, Atmospheric Environment. 56 (2012) 1–8. https://doi.org/10.1016/j.atmosenv.2012.03.079.

[29] O. Abida, M. Kolar, J. Jirkovsky, G. Mailhot, Degradation of 4-chlorophenol in aqueous solution photoinduced by Fe(III)-citrate complex, Photochem Photobiol Sci. 11 (2012) 794–802. https://doi.org/10.1039/c2pp05358f.

[30] R.E. Hamm, Complex Ions of Chromium. IV. The Ethylenediaminetetraacetic Acid Complex with Chromium(III)1, ACS Publications. (2002). https://doi.org/10.1021/ja01118a059.

[31] D. Jia, S.-P. Sun, Z. Wu, N. Wang, Y. Jin, W. Dong, X.D. Chen, Q. Ke, TCE degradation in groundwater by chelators-assisted Fenton-like reaction of magnetite: Sand columns demonstration, Journal of Hazardous Materials. 346 (2018) 124–132. https://doi.org/10.1016/j.jhazmat.2017.12.031.

[32] J. He, X. Yang, B. Men, L. Yu, D. Wang, EDTA enhanced heterogeneous Fenton oxidation of dimethyl phthalate catalyzed by Fe_3O_4: Kinetics and interface mechanism, Journal of Molecular Catalysis A: Chemical. 408 (2015) 179–188. https://doi.org/10.1016/j.molcata.2015.07.030.

[33] M. Gracheva, Z. Homonnay, A. Singh, F. Fodor, V.B. Marosi, Á. Solti, K. Kovács, New aspects of the photodegradation of iron(III) citrate: spectroscopic studies and plant-

related factors, Photochem Photobiol Sci. (2022). https://doi.org/10.1007/s43630-022-00188-1.

[34] C. Du, Y. Zhang, Z. Zhang, L. Zhou, G. Yu, X. Wen, T. Chi, G. Wang, Y. Su, F. Deng, Y. Lv, H. Zhu, Fe-based metal organic frameworks (Fe-MOFs) for organic pollutants removal via photo-Fenton: A review, Chemical Engineering Journal. 431 (2022) 133932. https://doi.org/10.1016/j.cej.2021.133932.

[35] V. Poza-Nogueiras, Á. Moratalla, M. Pazos, Á. Sanromán, C. Sáez, M.A. Rodrigo, Exploring the pressurized heterogeneous electro-Fenton process and modelling the system, Chemical Engineering Journal. 431 (2022) 133280. https://doi.org/10.1016/j.cej.2021.133280.

[36] Y. Zhang, X. Chen, M.-S. Cui, Z. Guo, Y.-H. Chen, K.-P. Cui, Z.-G. Ding, R. Weerasooriya, Binding Fe-doped g-C_3N_4 on the porous diatomite for efficient degradation of tetracycline via photo-Fenton process, Journal of Environmental Chemical Engineering. 10 (2022) 107406. https://doi.org/10.1016/j.jece.2022.107406.